Int. J. Multiphase Flow Vol. 7, No. 6, pp. 595–617, 1981
Printed in Great Britain.

0301-9322/81/060595-23$02.00/0
Pergamon/Elsevier

ANALYSIS OF TWO-PHASE FLOW MAGNETOHYDRODYNAMIC GENERATOR PERFORMANCE IN TERMS OF FLOW AND ELECTRICAL CONDUCTIVITY DISTRIBUTION PARAMETERS

FLAVIO DOBRAN
32-50, 34 St., Long Island City, NY 11106, U.S.A.

(*Received* 12 *September* 1980; *in revised form* 23 *March* 1981)

Abstract—A general method is presented for analyzing two-phase flow in magnetohydrodynamic generators. The method utilizes the time and flow-area-averaged kinematic, dynamic and electromagnetic quantities, and develops prediction capabilities of the generator performance parameters in terms of two fundamental physical parameters. These parameters are the flow and the electrical conductivity–flow distribution coefficients. The flow coefficient takes into consideration flow and relative velocity distribution, and the electrical conductivity–flow coefficient expresses the distribution of electrical conductivity with flow at any cross-sectional area of the generator duct.

The flow and electrical conductivity–flow distribution coefficients depend primarily on the two-phase flow regime and on the ratio of volumetric flow rates of the two phases in the duct. This conclusion has been established by examining the experimental data. Examination of the experimental data has also revealed the values of these coefficients for bubbly and churn–turbulent flow regimes for the wide range of ratios of volumetric flow rates. The analysis develops expressions for two–phase MHD generator load factor, electromagnetic pressure distribution across and along the generator channel, the distribution of the electromagnetic fields and interaction parameter.

1. INTRODUCTION

Energy conversion systems which utilize two-phase flow magnetohydrodynamic generator show a promising concept (Petrick 1976, Pierson *et al.* 1979). In the envisioned thermodynamic cycles the two-phase mixture of liquid metal and gas is caused to expand through the magnetohydrodynamic (MHD) generator duct. Liquid metal is the electrodynamic fluid and the gas acts as a pump for the liquid.

Liquid metal is heated to the desired operating temperature in solar collectors, nuclear reactors or by conventional fuels. Before entering the MHD duct, liquid metal is mixed in the mixer with the cooler gas where the gas is brought to the liquid metal temperature. The mixture of liquid metal and gas is next caused to cross the lines of a transverse magnetic field in the MHD generator as a result of which a significant pressure gradient is established in the flow. The pressure gradient causes gas to expand and preferably all of its mechanical energy of expansion is utilized to accelerate (pump) the liquid metal through the generator. The movement of liquid metal across magnetic field lines produces the current in the fluid which is utilized through an external electrical load. Because of the large thermal capacity of liquid metal, the expansion of two-phase mixture is nearly isothermal and, therefore, desirable since the cycle can approach the Carnot cycle efficiency. After expansion the liquid metal is pumped to the heat source and the gas, still at high temperature, can be further expanded in the gas turbine.

The performance of two-phase flow liquid metal magnetohydrodynamic (TFMHD) generator critically depends on the distribution of phases. Since the gas phase acts as a pump for the liquid metal, any significant relative velocity between the phases brings about a decrease in the generator performance. With the expansion of the gas phase along the generator duct, the void fraction increases with the resultant increase in the relative velocity between the gas and the liquid metal.

Recently, experiments have been carried out by Saito *et al.* (1978) with a two-phase mixture of NaK–N_2 with strong applied (transverse to the main flow) magnetic field to determine the field effect on the distribution of phases. The experiments clearly demonstrate the redistribution

of the concentration profile that is brought about by the *induced* magnetic field along the main flow direction. It is shown that at low applied magnetic fields gaseous concentration (void fraction) has the highest concentration near the duct axis. With the increase in the value of the applied field the void fraction peaks closer to the generator walls.

The unsteadiness of the two-phase mixture parameters makes it difficult to interpret the experimental data unless these parameters are given meaningful physical definition. In order to compare experimental data and present TFMHD generator performance characteristics it is necessary to define physically meaningful two-phase flow parameters. In an ordinary two-phase flow the above procedure has been standard for some time. However, in TFMHD flow only recently has some attempt been made by Saito *et al.* (1978) to present the data from the experiment in the above-mentioned form.

Purpose of the paper

It is the purpose of this paper to present a general method for the analysis of one-dimensional two-phase flow in MHD generators. This presentation is possible in light of the recent formulation of magnetohydrodynamic two-phase flow by Dobran (1981). The analysis presented herein takes into account the non-uniform flow distribution, relative velocity distribution, and the non-uniform distribution of electrical conductivity due to the non-uniform distribution of flow by means of two distribution parameters. It is then shown how these flow and electrical conductivity–flow distribution parameters affect the generator performance characteristics under a transversely (to the main flow) applied magnetic field. In view of the recently published experimental data, it is also demonstrated how these parameters can be determined from the experiment. One important characteristic in the analysis is also the introduction of time correlation. For this reason the development presented below goes beyond the development of ordinary two-phase flow distribution parameters.

2. PREVIOUS WORK

In ordinary two-phase flow, Zuber & Findlay (1965) were the first to show, in an elegant manner, how the flow distribution, concentration distribution and the distribution of relative velocity of the two-phase mixture can be taken into account when reducing the experimental data. Their basic approach was to start from local velocity fields, flow cross-sectional area averaging these fields, and defining the void fraction weighted mean quantities. Thus the dispersed flow weighted mean velocity was expressed by

$$\ll V_d \gg = \frac{\langle\!\langle \alpha_d V_d \rangle\!\rangle}{\langle\!\langle \alpha_d \rangle\!\rangle} = \frac{\langle\!\langle J_d \rangle\!\rangle}{\langle\!\langle \alpha_d \rangle\!\rangle} \equiv C_0 \langle\!\langle J \rangle\!\rangle + \frac{\langle\!\langle \alpha_d V_{dj} \rangle\!\rangle}{\langle\!\langle \alpha_d \rangle\!\rangle}, \qquad [1]$$

where J_d is local volumetric flux of the dispersed phase; J is the local total volumetric flux; V_{dj} is the drift velocity; and C_0 is the distribution parameter defined by

$$C_0 \equiv \frac{\langle\!\langle \alpha_d J \rangle\!\rangle}{\langle\!\langle \alpha_d \rangle\!\rangle \langle\!\langle J \rangle\!\rangle} = \frac{\frac{1}{a}\int_a \alpha_d J \, da}{\left[\frac{1}{a}\int_a \alpha_d \, da\right]\left[\frac{1}{a}\int_a J \, da\right]}. \qquad [2]$$

The averaging operator $\langle\!\langle \rangle\!\rangle$ represents the area-average and is defined by [11]. It was further shown by Zuber & Findlay, that the ratio of dispersed phase weighted mean velocity to the continuous phase weighted mean velocity can be expressed as

$$S \equiv \frac{\ll V_d \gg}{\ll V_c \gg} = \frac{\langle\!\langle 1 - \alpha_d \rangle\!\rangle}{\dfrac{1}{C_0 + \dfrac{\langle\!\langle \alpha_d V_{dj} \rangle\!\rangle}{\langle\!\langle \alpha_d \rangle\!\rangle \langle\!\langle J \rangle\!\rangle}} - \langle\!\langle \alpha_d \rangle\!\rangle}. \qquad [3]$$

Knowledge of the void fraction profiles and constitutive relations for the drift velocity has allowed the above authors to present a general framework for the classification of flow regimes in terms of the distribution parameter C_0 and the relative velocity parameter

$$\frac{\langle \alpha_d V_{dj} \rangle}{\langle \alpha_d \rangle}.$$

Recently Saito *et al.* (1978) have attempted a similar analysis for MHD flow through the generator duct. Apparently unaware of the Zuber & Findlay work, they introduced two parameters, K_1 and K_2, viz.

$$K_1 \equiv \frac{\langle \alpha_d V \rangle}{\langle \alpha_d \rangle \langle V \rangle}, \qquad K_2 \equiv \frac{\langle \sigma_t V \rangle}{\langle \sigma_t \rangle \langle V \rangle}. \qquad [4,5]$$

V is the velocity of gas or liquid and σ_t is the two-phase homogeneous mixture electrical conductivity assumed to be in the form

$$\sigma_t = \sigma_s(1 - 1.1\alpha_d). \qquad [6]$$

It therefore follows that

$$K_2 = \frac{1 - 1.1K_1\langle \alpha_d \rangle}{1 - 1.1\langle \alpha_d \rangle}. \qquad [7]$$

The experimental data agreed very well with the theory when the value of $K_1 = 1.3$ is chosen. This agreement is in the velocity ratio, load factor and pressure distribution. It should be noted that this agreement is between the total measured pressure gradient and electrodynamic pressure gradient computed from theory. For the flows with negligible drift velocity, $|V_{dj}| \ll |V_d|$, $V_d = J = V_c = V$ and, therefore, K_1 can be identified with the Zuber & Findlay distribution parameter C_0. As to why the experiment and theory in the analysis of Saito *et al.* agree with each other well under the drastic assumption of negligible drift velocity in the formulation, requires the consideration of a consistent theoretical framework of TFMHD presented below.

3. ANALYSIS

The two-phase flow model

Dobran (1981) formulated a general theory of two-phase magnetohydrodynamic flow applicable also to the flow in a variable area duct. Formulation of the flow model is carried out by the flow cross-sectional area and time averaging of the basic conservation equations of mass, momentum, energy and electromagnetic field for each phase. By defining the void fraction weighted mean properties, the conservation equations for fluid flow and electromagnetic field describing the two-fluid model and the mixture model have been obtained.

Time averaging is carried out over an interval of time $[t]$. The time associated with phase k (dispersed or continuous) at a point in space is denoted by $[t]_k$, and since the formulation assumes that the interface between the phases is a surface of discontinuity, $[t] = [t]_d + [t]_c$. Denoting

$$x_k(\mathbf{x}, t) = 1 \text{ if point } \mathbf{x} \text{ pertains to phase } k$$
$$= 0 \text{ if point } \mathbf{x} \text{ does not pertain to phase } k,$$

the time average over $[t]_k$ of a phase property F_k is defined by

$$\bar{F}_k^{x_k} \equiv \frac{1}{[t]_k} \int_{[t]} x_k F_k \mathrm{d}t, \tag{8}$$

and the time average void fraction at a point in space **x** by

$$\alpha_k \equiv \frac{[t]_k}{[t]}. \tag{9}$$

The time average of F_k is thus expressed by

$$\bar{F}_k \equiv \frac{1}{[t]} \int_{[t]} F_k \mathrm{d}t. \tag{10}$$

Defining next the area-averaged operator by

$$\nmid \nmid \equiv \frac{1}{a} \int_a \mathrm{d}a, \tag{11}$$

it is proved that the time-average of the area-averaged quantity is equal to the area-average of the time-averaged quantity.† Thus

$$\nmid \alpha_k \bar{F}_k^{x_k} \nmid = \nmid \bar{F}_k \nmid = \frac{1}{a} \overline{a_k < F_k >},$$

where $< >$ is the area-average over a_k. The void fraction weighted mean value is defined by

$$\ll F_k \gg \equiv \frac{\nmid \alpha_k \bar{F}_k^{x_k} \nmid}{\nmid \alpha_k \nmid}. \tag{12}$$

Basic kinematic relations and the definition of flow distribution parameters

Examination of the conservation of mass equation for the two-phase mixture (Dobran 1981) results in the definition of mixture density

$$\varphi_m \equiv \nmid \alpha_d \nmid \ll \varphi_d \gg + (1 - \nmid \alpha_d \nmid) \ll \varphi_c \gg \tag{13}$$

and mixture velocity

$$\mathbf{V}_m \equiv \frac{1}{\varphi_m} (\nmid \alpha_d \nmid \ll \varphi_d \mathbf{V}_d \gg + (1 - \nmid \alpha_d \nmid) \ll \varphi_c \mathbf{V}_c \gg). \tag{14}$$

The velocity of the center of volume is expressed by

$$\nmid \bar{\mathbf{J}} \nmid = \nmid \bar{\mathbf{J}}_d \nmid + \nmid \bar{\mathbf{J}}_c \nmid = \nmid \alpha_d \nmid \ll \mathbf{V}_d \gg + (1 - \nmid \alpha_d \nmid) \ll \mathbf{V}_c \gg, \tag{15}$$

and the *dispersed phase drift velocity* by

$$\bar{\mathbf{V}}_{dj} \equiv \ll \mathbf{V}_d \gg - \nmid \bar{\mathbf{J}} \nmid = (1 - \nmid \alpha_d \nmid)(\ll \mathbf{V}_d \gg - \ll \mathbf{V}_c \gg), \tag{16}$$

†This is true only if the regularity conditions on the integral operators hold.

when [15] is utilized. Utilizing [14], [16] and assuming that the covariance term

$$\mathrm{cov}(\alpha_k\varphi_k\mathbf{V}_k) \equiv \nmid\alpha_k\nmid \ll \varphi_k\mathbf{V}_k \gg - \nmid\alpha_k\nmid \ll \varphi_k \gg \ll \mathbf{V}_k \gg$$

is zero,† the following expressions are obtained:

$$\mathbf{V}_m = \frac{1}{\varphi_m}(\nmid\alpha_d\nmid\varphi_d \ll \mathbf{V}_d \gg + (1 - \nmid\alpha_d\nmid)\varphi_c \ll \mathbf{V}_c \gg) \qquad [17]$$

$$\ll \mathbf{V}_c \gg = \mathbf{V}_m - \frac{\varphi_d \nmid\alpha_d\nmid}{\varphi_m(1 - \nmid\alpha_d\nmid)}\tilde{\mathbf{V}}_{dj} \qquad [18]$$

$$\ll \mathbf{V}_d \gg = \mathbf{V}_m + \frac{\varphi_c}{\varphi_m}\tilde{\mathbf{V}}_{dj}. \qquad [19]$$

The *weighted mean drift velocity* is obtained by time and area averaging of $\mathbf{V}_{dj} = \mathbf{V}_d - \mathbf{J}$, leading to

$$\ll \mathbf{V}_{dj} \gg = \ll \mathbf{V}_d \gg - \frac{\nmid\alpha_d\bar{\mathbf{J}}^{x_d}\nmid}{\nmid\alpha_d\nmid}. \qquad [20]$$

Identifying the z direction as the main flow direction in the generator, figure 1, [20] is rewritten as

$$\ll w_d \gg = \ll w_{dj} \gg + C_0\nmid\bar{J}\nmid, \qquad [21]$$

where $w = \mathbf{V} \cdot \hat{n}_z$, $J = \mathbf{J} \cdot \hat{n}_z$ and

$$C_0 \equiv \frac{\nmid\alpha_d\bar{J}^{x_d}\nmid}{\nmid\alpha_d\nmid\nmid\bar{J}\nmid}. \qquad [22]$$

Using [21], [16] becomes

$$w_{dj} = \ll w_{dj} \gg + (C_0 - 1)\nmid\bar{J}\nmid, \qquad [23]$$

where $w_{dj} = \tilde{\mathbf{V}}_{dj} \cdot \hat{n}_z$.

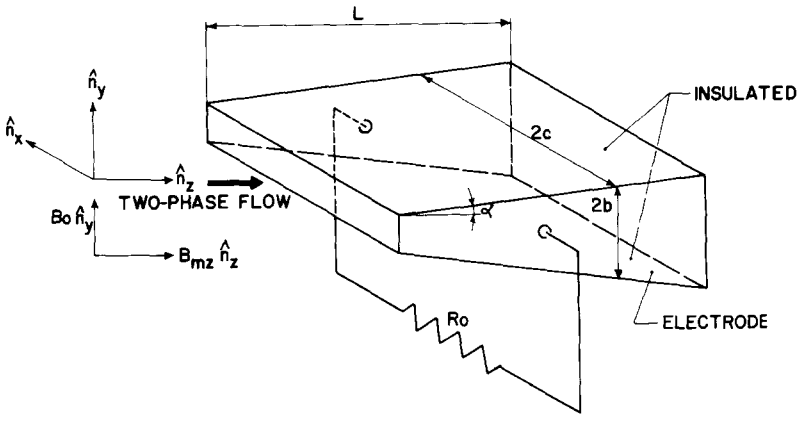

Figure 1. Two-phase flow in a magnetohydrodynamic channel.

†This is true if either the density or velocity has a flat profile. In the MHD generator, the density is expected to have flat profile due to the near isothermal flow and small pressure gradient transverse to the main flow.

Equations [21] and [22] are identical to Zuber and Findlay's [1] and [2] except for one important difference. This difference results from the time averaging in addition to area averaging in the present analysis and is most visible in the distribution parameter C_0. The definition of distribution parameter, [22], takes into account not only the effect of non-uniform flow and concentration profile in the duct but also the time correlation of this flow distribution. This is a novel feature, apparently unrecognized in all previous analyses. The effect of the relative velocity between phases is expressed by the weighted mean drift velocity $\ll w_{dj} \gg$.

The continuous phase drift velocity is by definition equal to

$$\tilde{\mathbf{V}}_{cj} \equiv \ll \mathbf{V}_c \gg - \not\langle \bar{\mathbf{J}} \not\rangle , \tag{24}$$

and using [15] and [16] it becomes

$$\tilde{\mathbf{V}}_{cj} = - \not\langle \alpha_d \not\rangle \frac{\tilde{\mathbf{V}}_{dj}}{(1 - \not\langle \alpha_d \not\rangle)} . \tag{25}$$

Defining the *velocity ratio* or *slip* by

$$S = \frac{\ll w_d \gg}{\ll w_c \gg} ,$$

and using [21] and [23]–[25] the following is obtained:

$$S = \frac{1 - \not\langle \alpha_d \not\rangle}{\dfrac{1}{K_f} - \not\langle \alpha_d \not\rangle} , \tag{26a}$$

where the *flow distribution coefficient* is given by

$$K_f \equiv C_0 + \frac{\ll w_{dj} \gg}{\not\langle \bar{J} \not\rangle} . \tag{26b}$$

Equation [26a] is similar to the Zuber & Findlay's [3].

An expression for the dispersed phase concentration profile can be obtained from [21] and the knowledge of dispersed phase volumetric flux

$$\not\langle \alpha_d \not\rangle = \frac{\not\langle \bar{J}_d \not\rangle}{\ll w_d \gg} = \frac{\not\langle \bar{J}_d \not\rangle}{K_f \not\langle \bar{J} \not\rangle} \tag{27}$$

or in terms of the two-phase mixture quality. The latter is more convenient for the analysis of two-phase MHD generator since the mixture is non-reacting and, therefore, the quality remains uniform along the duct length in steady flow. From the consideration of continuity equations of two phases (Dobran 1981), the dispersed and continuous phase mass flow-rates are:

$$M_d = a \not\langle \alpha_d \not\rangle \varphi_d \ll w_d \gg \tag{28a}$$

and

$$M_c = a(1 - \not\langle \alpha_d \not\rangle)\varphi_c \ll w_c \gg . \tag{28b}$$

Utilizing [26], [28] and the definition of quality

$$X \equiv \frac{M_d}{M_d + M_c}$$

it follows that the void fraction is equal to

$$\langle\!\langle \alpha_d \rangle\!\rangle = \frac{\beta}{(1+\beta)K_f} = \frac{\beta}{S+\beta}, \qquad [29]$$

where

$$\beta \equiv \frac{X}{1-X}\frac{\varphi_c}{\varphi_d}, \qquad [30]$$

and the velocity ratio is given by

$$S = K_f + \beta(K_f - 1). \qquad [31]$$

Since the value of S different from unity introduces loss of mechanical energy in the generator, it is seen from [31] that this loss is caused by three different mechanisms: The increase of β because of the significant decrease of gaseous phase density in the gas expansion through the generator; the flow distribution change along the generator duct; the relative velocity effect. If the relative velocity effect is minimized and the distribution parameter is kept close to unity, then the velocity ratio remains close to unity. A two-phase homogeneous flow is, therefore, preferred.

Distribution of electric, magnetic and pressure fields in the generator, and electrical conductivity–flow distribution parameter

Figure 1 illustrates the geometry of a typical two-phase flow MHD generator duct. The main flow direction is $\hat{n}_z$ and the *applied* magnetic field is in the direction $\hat{n}_y$ and considered constant. This results in the *induced* magnetic field to be in the direction $\hat{n}_z$. Since the two faces of generator, at $y = \pm b$, are insulated, the electric field vector is considered to be in the directions $\hat{n}_x$ and $\hat{n}_z$ only.

$$\mathbf{B} = B_0\hat{n}_y + B_z\hat{n}_z \qquad [32]$$

$$\mathbf{E} = E_x\hat{n}_x + E_z\hat{n}_z. \qquad [33]$$

Maxwell's electrodynamic equations for two-phase mixture have been derived by Dobran (1981) and are of the following form.

Faraday law:

$$\frac{\partial}{\partial z}(a\hat{n}_z \times \mathbf{E}_m) + \frac{\partial}{\partial t}(a\mathbf{B}_m) = -\sum_{k=d,c} \overline{\int_{C_k} \hat{n}_k \times \mathbf{E}_k \frac{d\zeta}{\hat{n}_k \cdot \hat{n}_{k\xi}}}. \qquad [34]$$

Ampere law:

$$\frac{\partial}{\partial z}(a\hat{n}_z \times \mathbf{B}_m) = \mu_0 a\mathbf{i}_m - \sum_{k=d,c} \overline{\int_{C_k} \hat{n}_k \times \mathbf{B}_k \frac{d\zeta}{\hat{n}_k \cdot \hat{n}_{k\xi}}} + \mu_0\epsilon_0 \overline{\int_{\xi_i} \sum_{k=d,c} \mathbf{E}_k\hat{n}_k \cdot \mathbf{S}_i \frac{d\zeta}{\hat{n}_k \cdot \hat{n}_{k\xi}}}, \qquad [35]$$

and the conditions

$$\frac{\partial}{\partial z}(a\hat{n}_z \cdot \mathbf{B}_m) = -\sum_{k=d,c} \overline{\int_{C_k} \hat{n}_k \cdot \mathbf{B}_k \frac{\mathrm{d}\xi}{\hat{n}_k \cdot \hat{n}_{k\xi}}} \qquad [36]$$

$$\frac{\partial}{\partial z}(a\hat{n}_z \cdot \mathbf{E}_m) = -\sum_{k=d,c} \overline{\int_{C_k} \hat{n}_k \cdot \mathbf{E}_k \frac{\mathrm{d}\zeta}{\hat{n}_k \cdot \hat{n}_{k\xi}}}. \qquad [37]$$

In above equations $\hat{n}_k$ is the unit vector normal to the surface of phase k at a cross-section of duct $a(z)$; $\hat{n}_{k\xi}$ is in the plane of $a(z)$ and is situated at the same point as $\hat{n}_k$; and C_k is the duct boundary perimeter which pertains to the phase k at the channel position z. $\mathbf{B}_m$ and $\mathbf{E}_m$ are mean magnetic and electric fields defined by

$$\mathbf{B}_m \equiv \not{\alpha}_d \not{\gg} \ll \mathbf{B}_d \gg + (1 - \not{\alpha}_d \not{\gg}) \ll \mathbf{B}_c \gg \qquad [38]$$

$$\mathbf{E}_m \equiv \not{\alpha}_d \not{\gg} \ll \mathbf{E}_d \gg + (1 - \not{\alpha}_d \not{\gg}) \ll \mathbf{E}_c \gg . \qquad [39]$$

Similarly, the mean current is defined by

$$\mathbf{i}_m \equiv \not{\alpha}_d \not{\gg} \ll \mathbf{i}_d \gg + (1 - \not{\alpha}_d \not{\gg}) \ll \mathbf{i}_c \gg , \qquad [40]$$

and utilizing the generalized Ohm's law without the Hall effect it is given by

$$\mathbf{i}_m = \not{\alpha}_d \not{\gg} \ll \sigma_d(\mathbf{E}_d + \mathbf{V}_d \times \mathbf{B}_d) \gg + (1 - \not{\alpha}_d \not{\gg}) \ll \sigma_c(\mathbf{E}_c + \mathbf{V}_c \times \mathbf{B}_c) \gg . \qquad [41]$$

In steady flow considered in this paper, [32]–[37] yield a number of important results for the distribution of electric and magnetic fields in the generator channel. For simplicity, it is considered that along any of the four segment perimeters of the channel, at a position z, the electric and magnetic fields assume constant values. This assumption provides ready treatment of integrals in [34]–[37].

From [34] it follows that $\hat{n}_x$ and $\hat{n}_z$ components yield respectively

$$(E_{wz})_{y=b} = (E_{wz})_{y=-b}, \quad (E_{wx})_{y=b} = (E_{wx})_{y=-b}, \qquad [42a,b]$$

and can be set equal to zero for the reference. The $\hat{n}_y$ component becomes (with condition [42b] assumed zero)

$$\frac{\partial E_{mx}}{\partial z} = -\frac{\tan\alpha}{b} E_{mx} + \frac{1}{2c}[(E_{wz})_{x=c} - (E_{wz})_{x=-c}] . \qquad [43a]$$

The channel divergence angle α is defined in figure 1 and should not be confused with the void fractions α_d and α_c. From the Ampere's law equation [35], the three components of the mean current vector are

$$i_{mx} = \frac{1}{2b\mu_0}[(B_{wz})_{y=b} - (B_{wz})_{y=-b}] \qquad [44]$$

$$i_{my} = -\frac{1}{2c\mu_0}[(B_{wz})_{x=c} - (B_{wz})_{x=-c}] \qquad [45]$$

$$i_{mz} = 0 , \qquad [46]$$

where the last term on the r.h.s. of [35] is assumed negligible. For a flat electric field profile this

assumption is rigorously justified. Conditions [36] and [37] require that

$$\frac{\partial B_{mz}}{\partial z} = -\frac{\tan\alpha}{b}\left[B_{mz} - \frac{(B_{wz})_{y=b} + (B_{wz})_{y=-b}}{2}\right] \qquad [47]$$

$$\frac{\partial E_{mz}}{\partial z} = -\frac{\tan\alpha}{b}E_{mz} - \frac{1}{2c}[(E_{wx})_{x=c} - (E_{wx})_{x=-c}]. \qquad [48]$$

Further simplification of [43]–[48] is possible by examining the generalized Ohm law equation [41]. Since in one-dimensional flow only the axial component of velocity in the generator is of significance, [41] yields

$$i_{my} = 0 \qquad [49a]$$

$$i_{mz} = \langle\!\langle \alpha_d \rangle\!\rangle \ll \sigma_d E_{dz} \gg + (1 - \langle\!\langle \alpha_d \rangle\!\rangle) \ll \sigma_c E_{cz} \gg \qquad [49b]$$

$$i_{mx} = \langle\!\langle \alpha_d \rangle\!\rangle \ll \sigma_d (E_{dx} - w_d B_0) \gg + (1 - \langle\!\langle \alpha_d \rangle\!\rangle) \ll \sigma_c (E_{cx} - w_c B_0) \gg . \qquad [50]$$

Equations [46] and [49b] imply that [43a] is given by

$$\frac{\partial E_{mx}}{\partial z} = -\frac{\tan\alpha}{b}E_{mx}. \qquad [43b]$$

Since usually $\tan\alpha/b \ll 1$, E_{mx} can be considered constant as a first approximation. From [48] the electric field is also constant on each electrode. The variation, along the axis of the generator channel, of the induced magnetic field is also expected to be of the second order with the proper compensation of the generator. i_{mx} is clearly not zero except in the unloaded state of the generator (open circuit condition).

To expound more clearly the effect of the induced magnetic field, it is necessary to examine the momentum equation for the two-phase mixture which has been derived by Dobran (1981) and written here without proof:

$$\begin{aligned}
&\frac{\partial}{\partial t}\left(a\sum_{k=d,c}\langle\!\langle \alpha_k \rangle\!\rangle \varphi_k \ll \mathbf{V}_k \gg\right) + \frac{\partial}{\partial z}\left(a\sum_{k=d,c}\langle\!\langle \alpha_k \rangle\!\rangle \varphi_k \ll \mathbf{V}_k w_k \gg\right) \\
&\quad = -\frac{\partial}{\partial z}(a\hat{n}_z P_m) + \frac{\partial}{\partial z}(a\hat{n}_z \cdot \boldsymbol{\pi}_m) + a\varphi_m \mathbf{g} \\
&\quad\quad + a\sum_{k=d,c}\langle\!\langle \alpha_k \rangle\!\rangle \ll \mathbf{i}_k \times \mathbf{B}_k \gg - \sum_{k=d,c}\overline{\int_{C_k} \hat{n}_k \cdot \mathbf{I}P_k \frac{\mathrm{d}\zeta}{\hat{n}_k \cdot \hat{n}_{k\xi}}} \\
&\quad\quad + \sum_{k=d,c}\overline{\int_{C_k} \hat{n}_k \cdot \boldsymbol{\pi}_k \frac{\mathrm{d}\zeta}{\hat{n}_k \cdot \hat{n}_{k\xi}}}.
\end{aligned} \qquad [51]$$

In this equation the mean pressure and mean viscous tensor are defined by

$$P_m \equiv \langle\!\langle \alpha_d \rangle\!\rangle \ll P_d \gg + (1 - \langle\!\langle \alpha_d \rangle\!\rangle) \ll P_c \gg \qquad [52]$$

$$\boldsymbol{\pi}_m \equiv \langle\!\langle \alpha_d \rangle\!\rangle \ll \boldsymbol{\pi}_d \gg + (1 - \langle\!\langle \alpha_d \rangle\!\rangle) \ll \boldsymbol{\pi}_c \gg . \qquad [53]$$

From [51] important information can be extracted on the distribution of axial and transverse pressure gradients.

If the acceleration, gravity and viscous effects are neglected then the pressure gradient must be balanced by electromagnetic forces, i.e.

$$(P_w)_{x=c} = (P_w)_{x=-c} \qquad [54]$$

$$(P_w)_{y=b} - (P_w)_{y=-b} = -2bi_{mx}B_{mz} \qquad [55]$$

$$\frac{\partial P_m}{\partial z} = B_0 i_{mx} - \frac{\tan\alpha}{b}\left[P_m - \frac{(P_w)_{y=b} + (P_w)_{y=-b}}{2}\right]. \qquad [56]$$

The pressure distribution at the wall described by [54]–[56] should be interpreted as the average values along the particular wall segment. The term in the square brackets in [56] is of the second order except for very high values of the applied magnetic field. From [55] it is clearly seen that the induced magnetic field brings about transverse-to-the-main-flow pressure variation. This transverse pressure gradient will influence the distribution of flow, distribution of concentration, distribution of relative velocities and the distribution of the effective electrical conductivity of the two-phase mixture.

In order to carry out the analysis further in a relatively straightforward manner, it will be assumed that the electric and magnetic fields have flat profiles. Equation [50] then is reduced to

$$i_{mx} = \sigma_m E_x - B_0[\not\langle \alpha_d \not\rangle \ll \sigma_d w_d \gg + (1 - \not\langle \alpha_d \not\rangle) \ll \sigma_c w_c \gg].$$

In this expression σ_m is the mean electrical conductivity defined by

$$\sigma_m \equiv \not\langle \alpha_d \not\rangle \ll \sigma_d \gg + (1 - \not\langle \alpha_d \not\rangle) \ll \sigma_c \gg . \qquad [57]$$

Introducing next the *electrical conductivity–flow correlation coefficients*

$$k_d \equiv \frac{\ll \sigma_d w_d \gg}{\ll \sigma_d \gg \ll w_d \gg}, \quad k_c \equiv \frac{\ll \sigma_c w_c \gg}{\ll \sigma_c \gg \ll w_c \gg}, \qquad [58a,b]$$

and utilizing [18] and [19], the mean electrical current becomes

$$i_{mx} = \sigma_m E_x - [\not\langle \alpha_d \not\rangle \ll \sigma_d \gg k_d + (1 - \not\langle \alpha_d \not\rangle) \ll \sigma_c \gg k_c] w_m B_0$$
$$- \frac{\not\langle \alpha_d \not\rangle w_{dj} B_0}{\varphi_m}[\varphi_c \ll \sigma_d \gg k_d - \varphi_d \ll \sigma_c \gg k_c]. \qquad [59]$$

It can be noted that the correlation coefficients introduced in [58] resemble [5]. However, the difference is twofold. Equation [5] assumes homogeneous flow and the local electrical conductivity for the mixture, whereas [58] do not. Equation [58a] can also be written as

$$k_d = \frac{\ll \sigma_d w_{dj} \gg}{\ll \sigma_d \gg \ll w_d \gg} + \frac{\not\langle \alpha_d \overline{\sigma_d J^{x_d}} \not\rangle}{\not\langle \alpha_d \not\rangle \ll \sigma_d \gg \ll w_d \gg},$$

and defining the distribution parameter of flow and electrical conductivity as

$$C_{d\sigma} \equiv \frac{\not\langle \alpha_d \overline{\sigma_d J^{x_d}} \not\rangle}{\not\langle \alpha_d \not\rangle \ll \sigma_d \gg \not\langle \bar{J} \not\rangle}, \qquad [60]$$

k_d is given by

$$k_d = \frac{C_{d\sigma} + \dfrac{\ll \sigma_d w_{dj} \gg}{\ll \sigma_d \gg \not\langle \bar{J} \not\rangle}}{K_f}. \qquad [61]$$

The correlation coefficient k_d in homogeneous flow (with $w_{dj} = 0$ and $C_0 = 1$) is considered to be

one.† In a similar manner the correlation coefficient for the continuous phase can be derived as

$$k_c = \frac{S}{K_f}\left(C_{c\sigma} + \frac{\ll \sigma_c w_{cj} \gg}{\ll \sigma_c \gg \not\langle \bar{J} \not\rangle}\right)$$
$$= \frac{K_f + \beta(K_f - 1)}{K_f} K_{cf}, \qquad [62a]$$

where the *electrical conductivity-flow distribution coefficient* (for the continuous phase) is given by

$$K_{cf} \equiv C_{c\sigma} + \frac{\ll \sigma_c w_{cj} \gg}{\ll \sigma_c \gg \not\langle \bar{J} \not\rangle}, \qquad [62b]$$

and where

$$C_{c\sigma} \equiv \frac{\not\langle \alpha_c \overline{\sigma_c J^{x_c}} \not\rangle}{\not\langle \alpha_c \not\rangle \ll \sigma_c \gg \not\langle \bar{J} \not\rangle}. \qquad [63]$$

The definition of electrical conductivity–flow distribution coefficient is similar to the definition of flow distribution coefficient and it also takes into consideration time correlation.

Generator performance parameters

In this section the MHD generator performance parameters are presented in terms of the distribution parameter, relative velocity parameter and the (continuous phase) conductivity–flow distribution coefficient. The values of these parameters are estimated from the available experimental data.

(a) *Flow distribution and relative velocity parameters.* Saito *et al.* (1978) and Petrick *et al.* (1976) carried out experiments in an MHD generator duct similar to figure 1 utilizing NaK–N_2 two-phase mixture. The dispersed phase is N_2 and the continuous phase is liquid metal NaK. Their data are especially useful for the determination of important flow distribution and conductivity–flow distribution parameters which have been derived in previous sections.

Figure 2 illustrates the data of Saito *et al.* (1978) and Petrick (1976) in a plot of the gas–liquid velocity ratio vs the gas–liquid volumetric flow ratio for various values of applied magnetic field and load resistances. The form of this plot is suggested by [31]. The data of Saito show no noticeable trend for differing values of magnetic field and load resistances. Petrick's data, however, show that in an unloaded generator the slip tends to be lower for higher values of β and higher for lower values of β from the loaded state of the generator. Comparing the slope and intercept of the line that linearly fits the data of Saito in figure 2 with [31] indicates that the flow coefficient is given by

$$K_f = C_0 + \frac{\ll w_{dj} \gg}{\not\langle \bar{J} \not\rangle} = 1.3. \qquad [64]$$

It is noted that Saito *et al.* identified this value with K_1 in [4] and that it is not necessarily equal to C_0 as stated by these authors. The relative constancy of the flow coefficient as given above indicates that any flow redistribution in the generator is compensated by the relative velocity change.

†Alternatively, a homogeneous flow can be defined such that $w_{dj} = 0$, $C_0 = 1$ and $k_d = k_c = 1$.

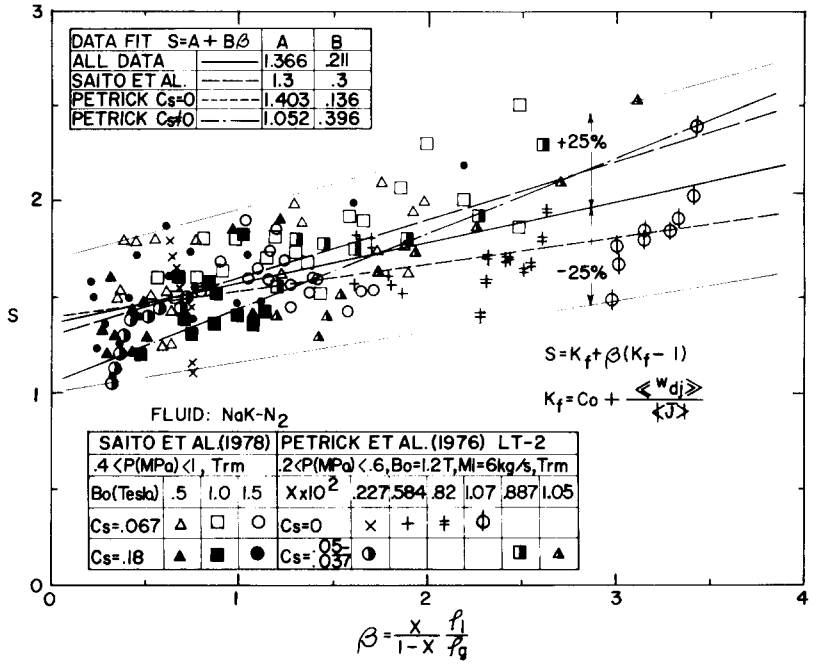

Figure 2. Correlation between gas-liquid velocity ratio and ratio of gas-liquid volumetric flow rates.

Petrick's data for the unloaded generator, $C_s = 0$, give

$$K_f = \frac{1.403 + 1.136\beta}{1 + \beta}, \qquad [65]$$

and for the loaded generator

$$K_f = \frac{1.052 + 1.396\beta}{1 + \beta}. \qquad [66]$$

The mass flow-rate of liquid metal never exceeded 7 kg/s in both sets of experiments in figure 2. The combined data of Saito and Petrick (1976) give

$$K_f = \frac{1.366 + 1.211\beta}{1 + \beta} \qquad [67a]$$

with a scatter of ± 20 per cent. This value of the flow coefficient can be accepted as representative of both sets of experiments. Also, since a typical change in β along the generator is on the order of one, it is possible to choose the slip for design purposes at an average value of β in the generator.

The recent data of Petrick *et al.* (1978) from LT-3 MHD generator and Pierson (1980) from HT-1 generator, are shown in figure 3. These data have a distinctly different character from the data of figure 2 except at low β where the trends are similar. Petrick (1978) attributes the differing character of these data due to the flow regime change brought about by the impurities in NaK-N_2 as a result of the revision of the two-phase flow facility at Argonne National Laboratory in 1976. From the experimental observation the flow regime in Figure 3 is identified as *bubbly* flow and the one in figure 2 as *churn-turbulent* flow. The former flow regime is more advantageous since it gives lower velocity ratios.

It is noted in figure 3 that bubbly flow gives lowest values of slip at higher values of β and at higher values of the liquid metal mass flow-rates. The future design of large scale MHD generators for commercial power generation will have to exploit this advantage. Also shown in

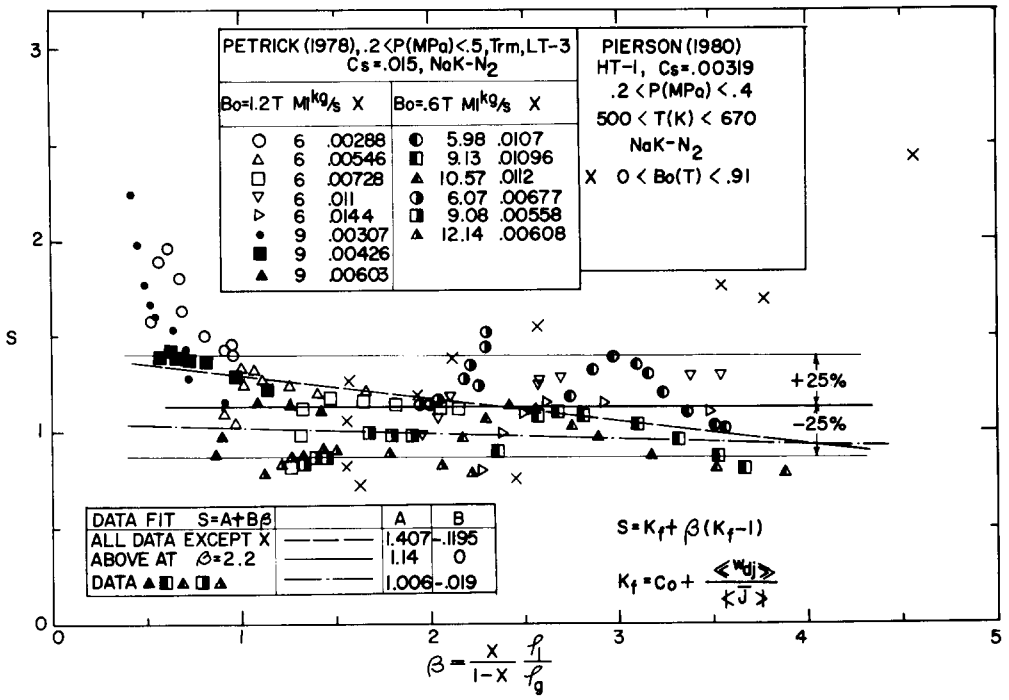

Figure 3. Correlation between gas–liquid velocity ratio and ratio of gas–liquid volumetric flow rates.

the same figure are the preliminary results from a high temperature NaK–N_2 facility at Argonne. These data appear to follow the trend of room temperature experiments. However, more experiments are required on the high temperature facility to more clearly establish the trend. Except at very low values of β, $\beta < 0.8$, a good data fit in figure 3 is $S = 1.14 \pm 25$ per cent. This gives the value of the flow factor as

$$K_f = \frac{1.14 + \beta}{1 + \beta}. \qquad [67b]$$

As much more data become available from the high temperature MHD facility, the flow coefficient should be correlated by the liquid metal mass flow-rate. Figure 3 shows that the data fit curve for high liquid mass flow-rates gives the slip very close to one.

Petrick *et al.* (1979) also carried out experiments in an LT-4 MHD generator which has been designed for high velocity (20 m/s) and high void fraction ($\alpha_d > 0.7$) operation. These data are shown in figure 4 where the *average* value of velocity ratio is plotted against the *average* value of β in the generator. The two extreme data points at $\beta = 7.63$ and at $\beta = 11.64$ cannot be attributed solely to the large value of void fraction since other data points represent large void fraction values also. The conclusion from the LT-4 experiments can be stated as follows: at large liquid mass flow-rates the velocity ratio approaches the data fit curve of LT-3 experiments whereas at low values of the liquid mass flow-rates, the velocity ratio approaches the LT-2 experiments and the data of Saito *et al.* Operating the generator of this type at low β and high liquid mass flow-rates leads to lower velocity ratios. Low β is achieved at lower qualities or/and lower values of φ_l/φ_g.

Some very careful future experiments are needed to more clearly delineate the effect of magnetic field strength and load resistance on the parameter K_f. The slight difference in the flow coefficient in the experiments of Saito & Petrick (1976) can be attributed to the method by which the gaseous phase is introduced into the liquid metal. An experimental program should be initiated to study the two-phase mixer designs, since the results would lead to a generator configuration with velocity ratios very close to one.

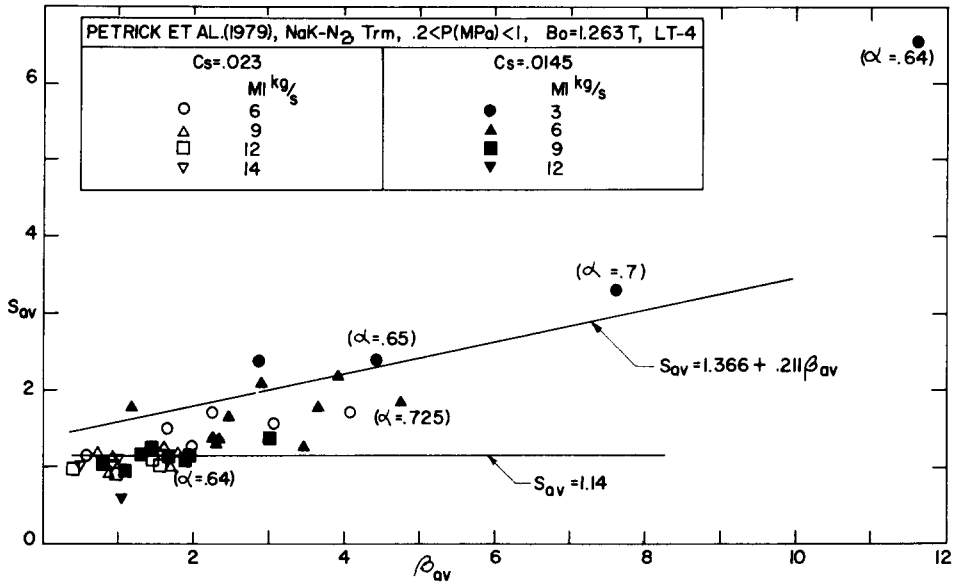

Figure 4. Correlation between the average gas–liquid velocity ratio and the average ratio of gas–liquid volumetric flow rates.

(b) *Generator load factor and the electrical conductivity–flow distribution coefficient.* If L is the length of the generator, R_0 the load resistance and Vt the voltage potential across the electrodes then

$$Vt = 2cE_x\,, \tag{68}$$

and

$$\frac{Vt}{LR_0} + 2bi_{mx} = 0\,. \tag{69}$$

The current density, i_{mx}, we can express in a more compact form by first noting that the drift velocity can be expressed as

$$\frac{w_{di}}{w_m} = \varphi_m \frac{(S-1)(1-\not\langle\alpha_d\not\rangle)}{\varphi_m + \varphi_d \not\langle\alpha_d\not\rangle (S-1)} \tag{70}$$

by using [23], [26], [15], [18] and [19]. Utilizing [70], [29] and [31], [59] becomes

$$i_{mx} = \sigma_m E_x - \frac{w_m B_0 \ll\sigma_c\gg k_c[K_f + \beta(K_f-1)]}{(1+\beta)K_f\left(1+\beta\dfrac{\varphi_d}{\varphi_c}\right)} \left(1+\frac{\beta\dfrac{\varphi_d}{\varphi_c}}{K_f+\beta(K_f-1)}\right)\left(1+\frac{\ll\sigma_d\gg}{\ll\sigma_c\gg}\frac{k_d}{k_c}\beta\right). \tag{71}$$

The voltage across the electrodes is thus

$$Vt = \frac{2cw_m B_0 \ll\sigma_c\gg k_c[K_f + \beta(K_f-1)]}{(1+Ct)\sigma_m(1+\beta)K_f\left(1+\beta\dfrac{\varphi_d}{\varphi_c}\right)} \left(1+\frac{\beta\dfrac{\varphi_d}{\varphi_c}}{K_f+\beta(K_f-1)}\right)\left(1+\frac{\ll\sigma_d\gg}{\ll\sigma_c\gg}\frac{k_d}{k_c}\beta\right), \tag{72}$$

where

$$Ct \equiv \frac{c}{\sigma_m b L R_0}$$

is the ratio of internal two-phase flow resistance to the external electrical circuit resistance.

The load factor is defined by

$$Kt^* \equiv \frac{E_x}{(E_x)_{\text{och}}}, \qquad [73]$$

where $(E_x)_{och}$ is the open circuit electric field ($i_{mx} = 0$) with homogeneous flow ($w_{dj} = 0$, $K_f = 1$), i.e. equal to $B_0 w_m$. Thus, the load factor based upon [62a], [68], [72] and [73] becomes

$$Kt^* = \frac{K_{cf}}{(1+Ct)} \frac{K_f + \beta(K_f - 1)}{K_f} \frac{\left(1 + \frac{\beta(\varphi_d/\varphi_c)}{K_f + \beta(K_f - 1)}\right)\left(1 + \frac{\ll \sigma_d \gg}{\ll \sigma_c \gg} \frac{k_d}{k_c} \beta\right)}{\left(1 + \frac{\ll \sigma_d \gg}{\ll \sigma_c \gg} \frac{\beta}{K_f + \beta(K_f - 1)}\right)\left(1 + \beta \frac{\varphi_d}{\varphi_c}\right)}, \qquad [74]$$

and

$$Ct = \frac{\sigma_s}{\ll \sigma_c \gg} \frac{Cs(1+\beta)K_f}{[K_f + \beta(K_f - 1)]\left[1 + \frac{\beta}{K_f + \beta(K_f - 1)} \frac{\ll \sigma_d \gg}{\ll \sigma_c \gg}\right]}, \qquad [75]$$

where σ_s is the electrical conductivity for single-phase flow in the generator and $Cs = c/(bR_0 L\sigma_s)$. For single-phase flow the load factor is equal to

$$Ks^* = \frac{1}{1+Cs},$$

and hence the ratio of the two-phase load factor to the single-phase flow load factor becomes

$$\frac{Kt^*}{Ks^*} = \frac{1+Cs}{1+Ct} \frac{K_f + \beta(K_f - 1)}{K_f} \frac{K_{cf}\left(1 + \frac{\beta(\varphi_d/\varphi_c)}{K_f + \beta(K_f - 1)}\right)\left(1 + \frac{\ll \sigma_d \gg}{\ll \sigma_c \gg} \frac{k_d}{k_c} \beta\right)}{\left(1 + \frac{\ll \sigma_d \gg}{\ll \sigma_c \gg} \frac{\beta}{K_f + \beta(K_f - 1)}\right)\left(1 + \beta \frac{\varphi_d}{\varphi_c}\right)}. \qquad [76]$$

Equation (76) allows the determination of electrical conductivity–flow distribution coefficient, K_{cf}, from the experimental data. For NaK–N_2 mixture the following conditions are clearly valid

$$\frac{\ll \sigma_d \gg}{\ll \sigma_c \gg} \ll 1, \quad \frac{k_d}{k_c} = \text{order (1)},$$

and [76] is simplified to

$$\frac{Kt^*}{Ks^*} = \frac{(1+Cs)K_{cf}}{\left[1 + \frac{Cs(1+\beta)K_f}{K_f + \beta(K_f - 1)}\right]} \frac{K_f + \beta(K_f - 1)}{K_f} \frac{\left(1 + \frac{\beta(\varphi_d/\varphi_c)}{K_f + \beta(K_f - 1)}\right)}{(1 + \beta(\varphi_d/\varphi_c))}. \qquad [77]$$

Equation [77] also assumes that $\sigma_s = \ll \sigma_c \gg$.

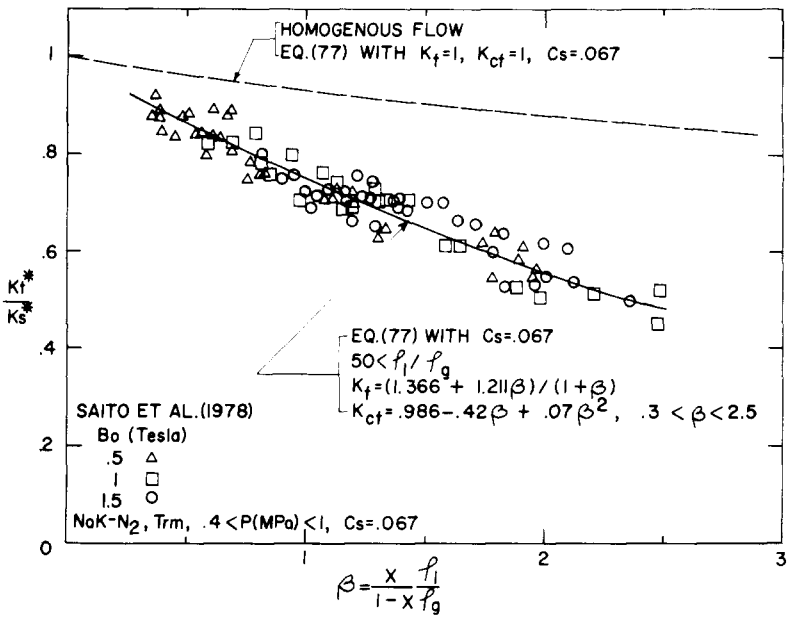

Figure 5. Correlation between the load factor and ratio of gas–liquid volumetric flow rates.

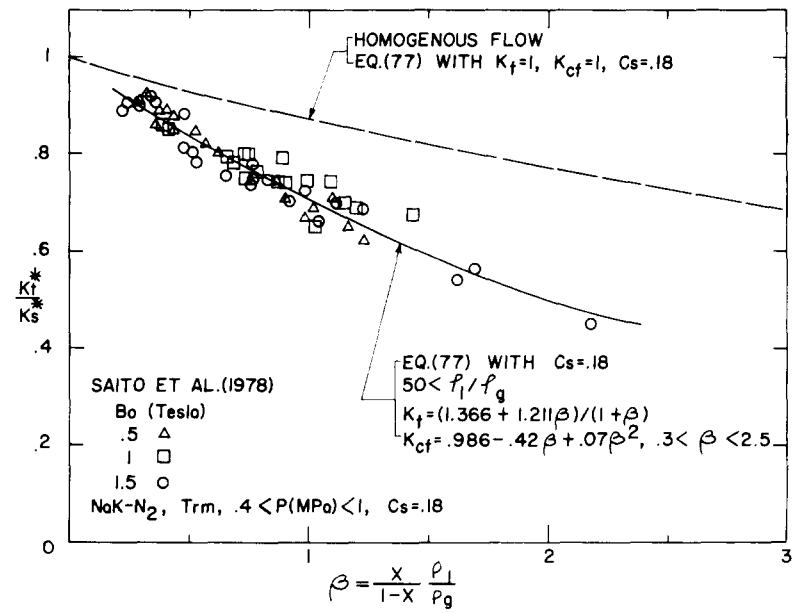

Figure 6. Correlation between the load factor and ratio of gas–liquid volumetric flow rates.

Figures 5 and 6 show the comparison between the experiments of Saito (1978) and [77] when the distribution coefficient of electrical conductivity–flow for the *churn-turbulent flow regime* is of the form

$$K_{cf} = 0.986 - 0.42\beta + 0.07\beta^2, \quad 0.3 < \beta < 2.5 . \qquad [78]$$

In figure 7 a comparison between the experimental data of Petrick *et al.* (1978) are made with the prediction of [77]. This indicates that the distribution coefficient of electrical conductivity–flow for the *bubbly flow regime* is as follows:

$$K_{cf} = 1.3 - 0.403\beta + 0.052\beta^2 , \quad 0.5 < \beta < 5 . \qquad [79]$$

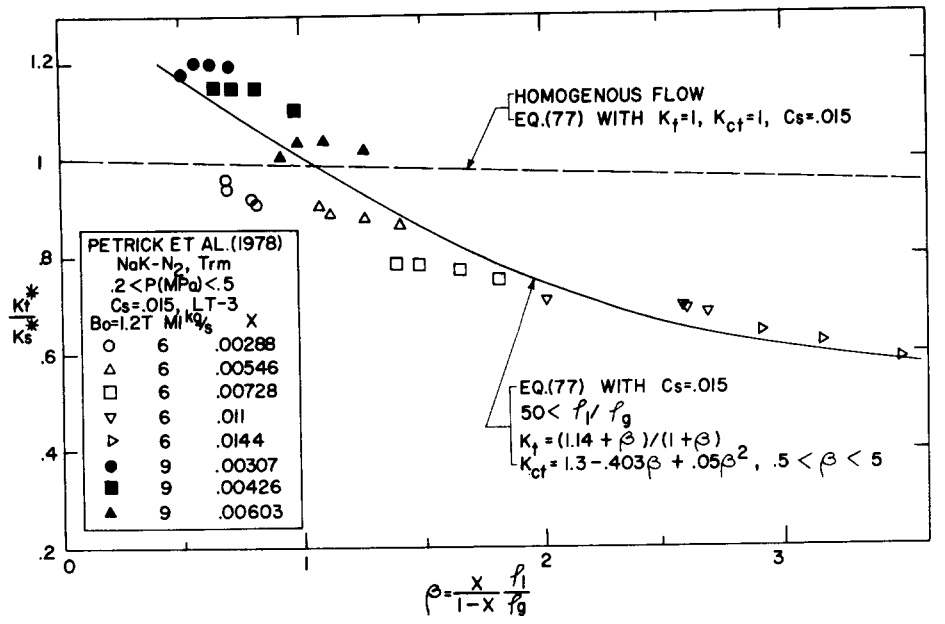

Figure 7. Correlation between the load factor and ratio of gas–liquid volumetric flow rates.

At low β in figure 7, the distribution coefficient K_{cf} for bubbly flow regime exceeds the value of one. Since for bubbly flow the slip ratio is close to one, [62b] shows that the electrical conductivity distribution parameter $C_{c\sigma}$ is larger than one. This implies that the void fraction α_d is larger close to the MHD duct centerline than close to the wall. For large β, $K_{cf} < 1$ and the opposite conclusion is valid. This shift of concentration profiles along the duct affects the mean current in the flow as can be seen by combining [71] and [74]. Near the duct inlet the circulating current aids the MHD power generation and causes pumping near the duct outlet. Control of the concentration profile across the duct cross-sectional area is thus very important for achieving efficient generator performance.

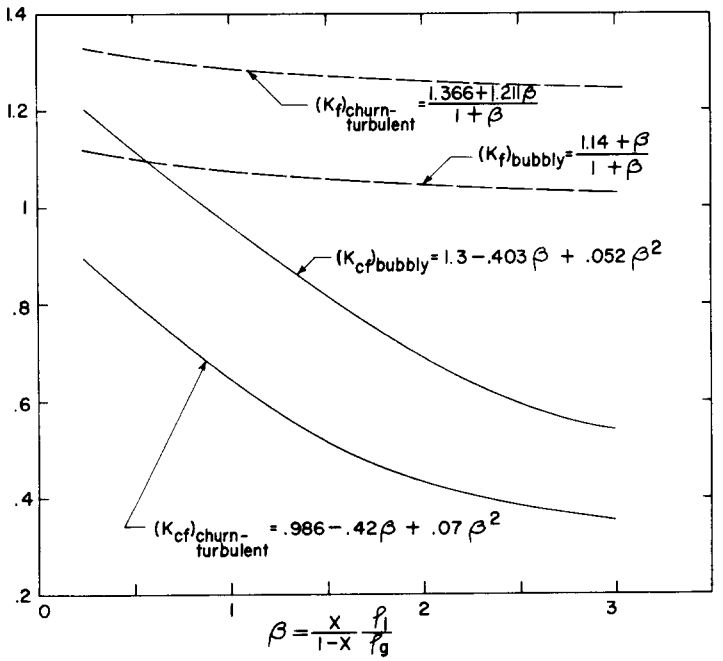

Figure 8. Comparison between flow and electrical conductivity–flow distribution coefficients for bubbly and churn–turbulent flow regimes.

(c) *Comparison of flow and electrical conductivity–flow distribution coefficients for bubbly and churn–turbulent flow regimes.* Figure 8 illustrates the comparison of distribution coefficients for bubbly and churn-turbulent flow regimes. In bubbly flow the flow coefficient, K_f, has a value closer to one than in churn-turbulent flow. This indicates that the sum of distribution and relative velocity parameters approaches unity. The electrical conductivity–flow distribution coefficient, K_{cf}, is also closer to one for the bubbly flow than for the churn–turbulent flow. Physically this is expected, since in bubbly flow the electrical conductivity for the two-phase mixture should have a profile which is nearly flat.

Referring to figure 8 it can be concluded that the following approximate relations are valid

$$(K_f)_{\text{churn-turbulent}} \cong (K_f)_{\text{bubbly}} + 0.21 \qquad [80]$$

$$(K_{cf})_{\text{bubbly}} \cong (K_{cf})_{\text{churn-turbulent}} + 0.3 \qquad [81]$$

for the range of $0.5 < \beta < 3$.

(d) *Electromagnetic pressure gradient distribution.* The distribution of pressure gradient due to the electromagnetic force is expressed by [56]. The second term on the r.h.s. of this equation can be neglected for it is negligible in comparison to the first term. Based on [68], [71] and [72], [56] becomes

$$\left(\frac{dP_m}{dz}\right)_t = -\frac{Ct}{(1+Ct)} \frac{B_0^2 w_m \ll \sigma_c \gg k_c [K_f + \beta(K_f - 1)]}{(1+\beta)K_f\left(1+\beta\frac{\varphi_d}{\varphi_c}\right)} \left(1+\frac{\beta\varphi_d/\varphi_c}{K_f+\beta(K_f-1)}\right)\left(1+\frac{\ll \sigma_d \gg}{\ll \sigma_c \gg}\frac{k_d}{k_c}\beta\right). \qquad [82]$$

Equation [82] can be normalized by the pressure gradient of the electromagnetic force in single-phase flow with the same applied magnetic field and continuous phase mass flow-rate as in two-phase flow. The result is:

$$\frac{\left(\frac{dP_m}{dz}\right)_t}{\left(\frac{dP}{dz}\right)_s} = \frac{1+Cs}{1+Ct} \frac{Ct \ll \sigma_c \gg \varphi_s k_c}{C_s \sigma_s \varphi_c} \left(1+\frac{\ll \sigma_d \gg k_d}{\ll \sigma_c \gg k_c}\beta\right). \qquad [83]$$

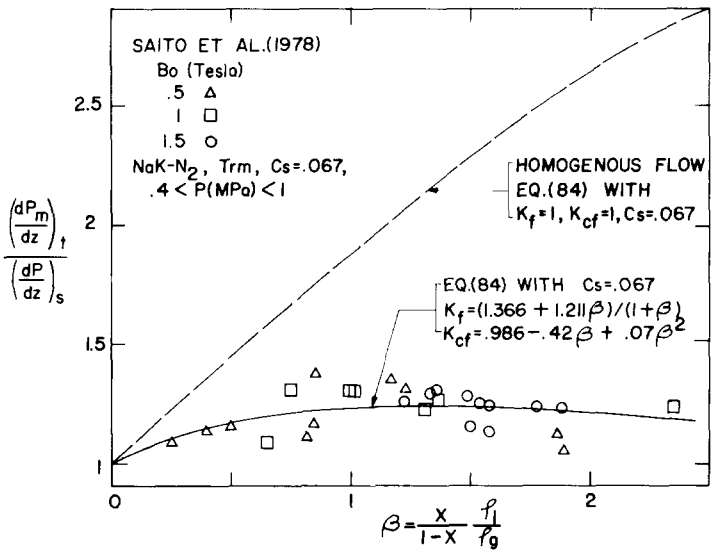

Figure 9. Correlation between the two-phase pressure gradient and ratio of gas–liquid volumetric flow rates.

In view of the approximations leading to [77], above relation is reduced to

$$\frac{\left(\frac{dP_m}{dz}\right)_t}{\left(\frac{dP}{dz}\right)_s} = \frac{1+Cs}{\left[1+\frac{Cs(1+\beta)K_f}{K_f+\beta(K_f-1)}\right]}(1+\beta)K_{cf}. \qquad [84]$$

Figures 9 and 10 compare the experimental data of Saito for the total pressure gradient with the prediction of [84]. In the reduction of data by these authors an incorrect expression was used to determine the single-phase velocity for the single-phase pressure gradient. The correct expression follows from [18], [31] and [70], and the requirement that

$$4bc\varphi_l w_s = 4bc(1-\nmid\alpha_d\nmid) \ll w_c \gg \varphi_c .$$

The reduced data in figures 9 and 10 bear this correction that is of the form

$$\frac{\left(\frac{dP}{dz}\right)_{s\text{—Saito}}}{\left(\frac{dP}{dz}\right)_{s\text{—this analysis}}} = \frac{K_f}{K_f+\beta(K_f-1)} \frac{\left(1+\beta\frac{\varphi_d}{\varphi_c}\right)}{\left(1+\frac{\beta\varphi_d/\varphi_c}{K_f+\beta(K_f-1)}\right)}.$$

As can be seen from figures 9 and 10, the two-phase electromagnetic pressure gradient compares very well with the *total* two-phase measured pressure gradient.

At high β it should be expected that the two-phase frictional pressure gradient is of importance and, therefore, the normalized pressure gradient expressed by [84] should fall below the data that represent the total two-phase pressure gradient that is normalized by the single-phase electromagnetic pressure gradient. The theoretical trend in figures 9 and 10 does not appear to follow the above explanation which indicates that the viscous pressure gradient is not significant in comparison to the electromagnetic pressure gradient at high values of applied magnetic fields and liquid metal mass flow rates below 7 kg/s.

(e) *Relationship between flow regimes and the induced magnetic field.* The relationship between the induced field and the flow regime can be expressed as a relationship between the

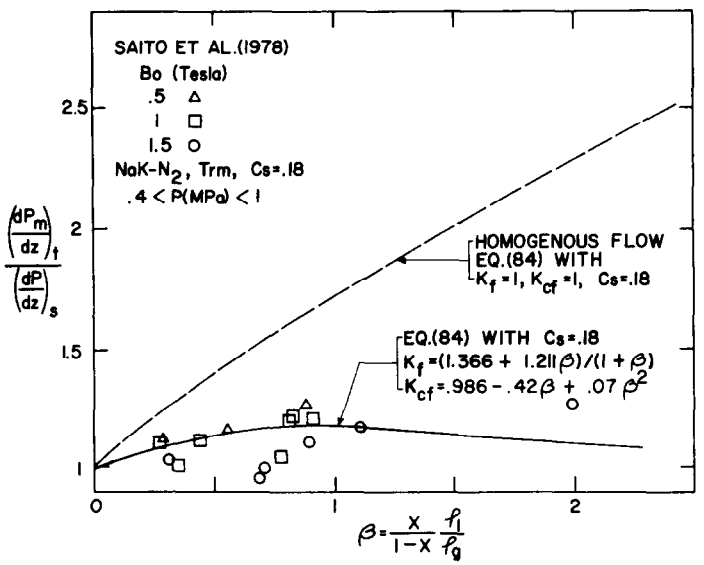

Figure 10. Correlation between the two-phase pressure gradient and ratio of gas–liquid volumetric flow rates.

magnetic interaction parameter and the electrical conductivity–flow distribution coefficient. To derive this relationship for two-phase flow, the single-phase flow analogy will be utilized for the definition of electromagnetic non-dimensional groups (Branover 1978).

The ratio of two-phase electromagnetic force due to the applied magnetic field (under zero potential difference) to the two-phase inertia force will be represented by the *magnetic interaction parameter for the applied magnetic field* No, i.e.

$$No = \left.\frac{bi_{mx}B_0}{\varphi_m w_m^2}\right|_{E_x=0}. \qquad [85]$$

The *magnetic Reynolds number* in two-phase flow, *Rm*, will be defined by the ratio of induced magnetic field to the applied magnetic field

$$Rm \equiv \frac{B_{mz}}{B_0} = \left.\frac{u_0 i_{mx} b}{B_0}\right|_{E_x=0}, \qquad [86]$$

and the *interaction parameter, Ni*, by the ratio of two-phase electromagnetic force due to the induced magnetic field to the two-phase inertia force. Hence

$$Ni = N_0 Rm = \left.\frac{\mu_0 b^2 i_{mx}^2}{\varphi_m w_m^2}\right|_{E_x=0}. \qquad [87]$$

On the basis of [71] and expressing φ_m in terms of β and K_f, the two-phase interaction parameter becomes

$$N_i = \frac{\mu_0 b^2 B_0^2 \ll \sigma_c \gg^2}{\varphi_c} \frac{\left(1+\dfrac{\beta\varphi_d/\varphi_c}{K_f+\beta(K_f-1)}\right)\left(1+\dfrac{\ll \sigma_d \gg}{\ll \sigma_c \gg}\dfrac{k_d}{k_c}\beta\right)^2}{(1+\beta\varphi_d/\varphi_c)^2(1+\beta)} \left(\frac{K_f+\beta(K_f-1)}{K_f}\right)^3 K_{cf}^2. \qquad [88]$$

Figure 11 shows the relationship between $Ni(\varphi_c/\mu_0 b^2 B_0^2 \ll \sigma_c \gg^2)$ and β for bubbly and churn–turbulent flow regimes. For fixed value of the applied magnetic field, the interaction parameter decreases with an increase in the ratio of volumetric flow rates of gas to liquid as is

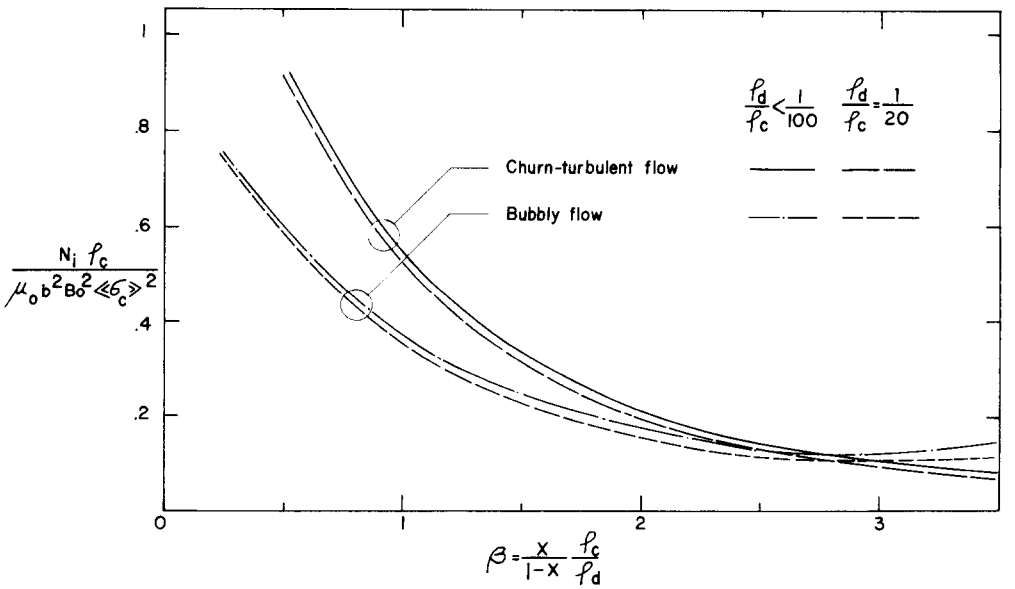

Figure 11. Relationship between the two-phase interaction parameter and the ratio of volumetric flow rates.

physically expected. For fixed values of B_0 and β, and at lower β, the interaction parameter has a lower value for the bubbly flow than for the churn–turbulent flow. This implies that the redistribution of flow is less severe in bubbly flow than in churn–turbulent flow for the same values of magnetic field and ratio of volumetric flow-rates. The effect of pressure in figure 11 is represented by the density ratio φ_d/φ_c. As can be seen this effect is not significant at low and medium pressures.

4. SUMMARY AND CONCLUSIONS

A general method has been presented for the analysis of two-phase non-reacting flow in a magnetohydrodynamic generator duct. Analysis of the two-phase flow was carried out by utilizing the one dimensional area and time-averaged form of the conservation equations. The analysis allows for the non-uniform distribution of phases and electrical conductivity across and along the generator duct, and as well as for the local slip between phases. The non-uniformities in concentration profile, local velocity ratio and electrical conductivity are expressed in terms of flow distribution and electrical conductivity–flow distribution coefficients. In the paper these distribution coefficients were determined from the experimental data and are found to depend primarily on the two-phase flow regime and on the ratio of volumetric flow rates of the two phases. The variation of the distribution coefficients along the generator duct is a result of the shift in the concentration profile across the duct cross-sectional area, and because of the increase of local relative velocity between the phases.

The flow regime significantly affects the MHD generator duct performance. Bubbly flow is preferable to other flow regimes. This gives lowest velocity ratios and the gas phase is optimally utilized to produce the pumping of liquid metal through the duct. The flow regime is a complex function of at least the following:

(1) Method of introducing the gaseous phase into the liquid metal (mixer design).
(2) Impurities in the two-phase mixture.
(3) Surface tension between the phases.
(4) The interaction parameter (magnetic field).
(5) Liquid metal mass flow-rate.

Examination of the experimental data has allowed the determination of flow distribution and electrical conductivity–flow distribution coefficients for bubbly and churn–turbulent flow regimes in a horizontal flow. It is also shown how the velocity ratio, load factor, electromagnetic pressure gradient and interaction parameter can be expressed in terms of these distribution coefficients. The load factor and electromagnetic pressure gradient correlate very well in terms of distribution coefficients. Some scatter of the experimental data exists and can be attributed to the complex flow interaction with the electromagnetic field at the inlet and outlet of the generator duct.

With knowledge of the distribution coefficients it is possible to construct a very detailed model of the two-phase flow field by solving the area and time-averaged form of the governing differential equations. The analytic determination of distribution coefficients requires statistical mechanics calculations which is not available at the present time. However, it is possible to determine the coefficients experimentally without recourse to the method presented in this paper.

Acknowledgement—The author would like to thank Dr. E. S. Pierson at Argonne National Laboratory for supplying the experimental data from high temperature two-phase flow MHD facility.

NOMENCLATURE

a area
b generator duct half height

$\mathbf{B}$ magnetic induction vector
B_0 applied magnetic field
c generator duct half width
C duct boundary perimeter
C_0 distribution parameter, defined by [22]
Cs single-phase load resistance parameter, defined by [75]
Ct two-phase load resistance parameter
$\mathbf{E}$ electric field vector
$\mathbf{g}$ gravitational force per unit mass
$\mathbf{i}$ electric current density
$\mathbf{I}$ unit tensor
$\mathbf{J}$ total volumetric flux
k correlation coefficient
K flow ór conductivity–flow distribution coefficient
Ks^* load factor for single-phase flow
Kt^* load factor for two-phase flow
L length of the generator channel
M mass flow rate
$\hat{n}_k$ unit normal vector
$\hat{n}_{x,y,z}$ unit vector in direction x, y, z respectively
Ni interaction parameter
p, P pressure
Re magnetic Reynolds number
R_0 external load resistance
S slip or velocity ratio of gas to liquid
$\mathbf{S}_i$ interface velocity
t time
Trm room temperature
$\mathbf{V}$ velocity vector
$\tilde{\mathbf{V}}_{dj}$ dispersed phase drift velocity
$\tilde{\mathbf{V}}_{cj}$ continuous phase drift velocity
Vt voltage across the generator electrodes
w axial flow velocity in the generator duct
$\mathbf{x}$ space vector
X quality

Greek symbols

α_k time-averaged void fraction, defined by [9]
α channel divergence angle defined in figure 1
β ratio of volumetric flow rates, defined by [30]
ϵ_0 dielectric permittivity of free space
μ_o magnetic permeability of free space
ξ perimeter
φ mass density
σ electrical conductivity
π viscous stress tensor

Subscripts

c continuous phase (liquid metal)
cf continuous phase conductivity–flow
d dispersed phase (gas)

f flow
g gas phase
i interface between phases
k denotes phase d and c, or g and l respectively
l liquid phase
m mean value
mx mean value x-component
my mean value y-component
mz mean value z-component
s single-phase
t two-phase
w wall of the generator duct
x, y, z duct coordinates, figure 1

Special symbols

$[t]$ averaging time interval
$< >$ area average operator, $1/a_k \int_{a_k} \mathrm{d}a$
$\{\!\{\ \}\!\}$ area average operator, $1/a \int_a \mathrm{d}a$
$\overline{\ }^{x_k}$ time average operator, $1/[t]_k \int_{[t]_k} \mathrm{d}t$
$\overline{\ }$ time average operator, $1/[t] \int_{[t]} \mathrm{d}t$
$\ll \gg$ void fraction weighted mean value operator, defined by [12]

REFERENCES

Branover, H. 1978 *Magnetohydrodynamic Flow in Ducts.* Wiley, New York.

Dobran, F. 1981 On the consistency conditions of averaging operators in two-phase flow models and on the formulation of magnetohydrodynamic two-phase flow. *Int. J. Engng Sci.* Will appear in 1981.

Petrick, M. 1976 Two-phase flow liquid metal MHD generator. In *MHD Flows and Turbulence, Proc. Bat-Sheva Int. Siminar.* Wiley, New York.

Petrick, M., Fabris, G., Pierson, E. S., Fisher, A. K. & Johnson, C. E. 1978 Experimental two-phase liquid metal magneto-hydrodynamic generator program. ANL/MHD-78-2.

Petrick, M., Fabris, G., Pierson, E. S., Fisher, A. K. Johnson, C. E., Gherson, P., Lykoudis, P. S. & Lynch, R. E. 1979 Experimental two-phase liquid metal magnetohydrodynamic generator program. ANL/MHD-79-1.

Pierson, E. S., Branover, H., Fabris, G. & Reed, C. B. 1979 Solar powered liquid metal MHD power systems. ASME Paper 79-WA/Sol-22.

Pierson, E. S. 1980 Experimental data from the high temperature two-phase flow MHD facility at Argonne National Laboratory. Personal communication.

Saito, M., Inoue, S. & Fujii-E, Y. 1978 Gas–liquid slip ratio and MHD pressure drop in two-phase liquid metal flow in a strong magnetic field. *J. Nucl. Tech.* **15**, 476–489.

Saito, M., Nagae, H., Inoue, S. & Fujii-E, Y. 1978 Redistribution of gaseous phase of liquid metal two-phase flow in a strong magnetic field. *J. Nucl. Tech.* **15**, 729–735.

Zuber, N. & Findlay, J. A. 1965 Average volumetric concentration in two-phase flow systems. *J. Heat Transfer* **87C**, 453–468.